GROUND-BASED GAMMA-RAY ASTRONOMY*

Ocker C. de Jager

Space Research Unit, Potchefstroom University for CHE
Potchefstroom 2520, South Africa
E-mail: okkie@fskocdj.puk.ac.za

(Received May 24, 1999)

This paper provides a brief review of ground-based γ-ray Astronomy. It is intended to discuss the basic observational techniques, technological constraints, and the advantages of going down in threshold energy. Some of the major discoveries are listed — galactic and extragalactic. We discuss some of the scientific returns as otained from observations of TeV sources such as the Crab nebula, shell remnants, and active galactic nuclei. Each source provides us with a richness of new physics, which prompt us to built larger telescopes and better photon detection devices to go down in threshold energy, so that ground-based observatories can overlap in energy with space observatories.

PACS numbers: 95.55.–n, 95.85.Pw

1. Introduction

Particle Astropysics is an extremely broad field, and cover topics on nuclear and other elementary particles as they occur in the universe. Whereas we are limited on Earth by the size of the accelerators, the unique conditions prevailing in cosmic sources allow us to reach the highest particle energies in the universe. The limitation from an Astroparticle viewpoint is that we cannot "order" reactions, as we do in the laboratory. We are therefore given a scenario by nature, and we have to identify what we are seeing. Once we have discovered a process in the cosmos, we may even predict where to see the process again, if we have gained sufficient understanding of what is going on. From the discussions below the reader will find that synchro-Compton processes dominate the detections of cosmic γ-ray sources. This is because the inverse Compton (IC) process is such an efficient mechanism to produce γ-rays, and if the source is not capable to provide a soft photon field acting as target for the IC process, the abundant 2.7K CMBR still provide an abundant source of target photons for this process.

* Presented at the XXVII International Meeting on Fundamental Physics, Sierra Nevada, Granada, Spain, February 1–5, 1999.

Technological breakthroughs allow us to improve the quality of observations, and this also define new windows on fundamental physics. The purpose of this lecture is to highlight some of the areas where we have made progress, and what type of information is gained from cosmic observations.

Cosmic ray studies is considered to be a branch of Particle Astrophysics, and X- and γ-ray Astronomy were inlcuded in Cosmic ray studies until significant breakthrough were made with the design of X-ray detectors. This resulted in the development of X-ray Astronomy as an independent branch of Astronomy, where the number of X-ray sources adds up to more than a million. Gamma-ray Astronomy, however, were slower to develop: Whereas ground-based γ-ray Astronomy struggled to produce convincing results, space-borne detectors had a relatively good start since the early 1970's with the launch of the SAS-2 detector, and later COS-B and CGRO instruments. The space-borne γ-ray observatories were able to reject a significant part of the background, but the angular resolution remains a problem. The latter property is important to resolve the positions of cosmic γ-ray emission.

Ground-based γ-ray Astronomy involves the placement of a detector at ground level. The incoming cosmic γ-ray (with energy well above a GeV) creates an electron-photon cascade, with a Čerenkov light pulse which is detectable at ground level. The pulse duration is a few nanoseconds, whereas the lateral distribution of the shower extends over a radius of about 200 meters. The failure to detect sources with confidence in the past was mainly due to the poor sensitivity of these detectors. Prior to the invention of the imaging technique (Weekes & Turver, 1977; Weekes *et al.* 1989), we had to rely on flux collectors rejecting only the night sky background, but none of the dominant charged cosmic ray induced showers. With several telescopes running now on the imaging principle, we can now identify sources with an angular resolution of 0.1 to 0.2 degrees. Ground-based γ-ray Astronomy therefore reached the level where it can identify new sources with significantly improved angular resolution compared to satellites, but the flux of photons is still small compared to γ-ray fluxes from sub GeV sources as seen by satellites.

The detection of γ-rays from cosmic sources can either be the result of accelerated charges producing high energy γ-rays, or, particles of a higher mass scale which decay to produce the observable γ-rays. This may include sources of γ-rays which involve non-standard physics. Astrophysical motivation for non-standard physics comes from the study of dark matter, as well as from the existence of cosmic rays with energies exceeding 10^{20} eV (Ong, 1998).

Since we are attempting to overlap the energy thresholds of space- and ground-based experiments, we have to be able to detect the weakest possible

signals with nanosecond resolution. This pushes the technology of photon detection devices to their limits. Whereas the present limit on the threshold of γ-ray detectors are around 100 GeV, there are attempts to move down to 10 GeV or even lower (see *e.g.* Barrio *et al.* 1998). This will however require the operation of high quantum efficiency devices such as avalanche photo diodes, but with lower noise levels compared to what is currently available on the market. Improved pre-amps for weak signals will also be required to reach new technological breakthroughs. Such breakthroughs also imply technological spinoffs which are useful for commercial applications.

A review of ground-based γ-ray Astronomy will be given, which will be followed by a brief review of the various types of sources which have been detected, with an emphasis on the physics that we learn from such observations.

2. The imaging atmospheric Čerenkov technique

It seems as if nature regulates the production of photons in cosmic sources, in the sense that there are many low energy photons, but very few photons of the highest energies. This gives some sort of "equipartition" between energies, which means that we should expect much less sources at TeV energies. This is no surprise, since we know of only a few TeV sources, and their fluxes are of the order of 10^{-11} photons.cm^{-2}.s^{-1}. To detect such a source within an hour, we clearly need a collection area of the order of $A_\gamma \sim 10^8 - 10^9$ cm^2, to give enough photons above the background of those cosmic ray showers which failed to be rejected by any imaging technique.

We are fortunate that γ-rays, upon entering the atmosphere of earth, produce Čerenkov flashes with a radii between 100 and 200 meters, so that collection areas of the order of 10^8 - 10^9 cm^2 are naturally reached. Detailed Monte Carlo studies of Čerenkov showers due to hadrons and γ-rays have been made by several authors using programs such as MOCCA, SIBYLL, CORSIKA and KASKADE (see Ong, 1998 for references and more detailed discussions). These programs agree on the 10–15% level (Ong, 1998), so that we expect to get consistent spectra for sources if measured by different experiments, unless systematic effects introduce offsets. Once a source has been detected, we can "easily" simulate the response of the γ-ray detector to incoming γ-rays, given the sensitivity of the photon detection device. This defines a collection area for showers above the threshold of detection, and hence a flux for the source. Observations of the Crab Nebula (see Fig. 1) by various groups resulted in converging flux measurements (within systematic uncertainties), which indicate that source physics can be seriously studied.

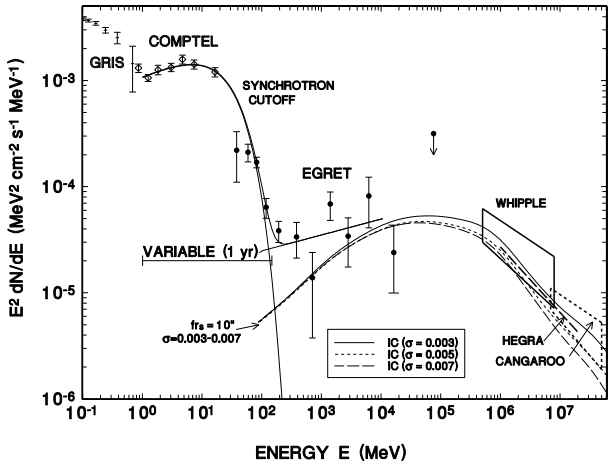

Fig. 1. The γ-ray spectrum of the Crab nebula from 100 keV to 5×10^{13} eV. The data below 30 GeV are from CGRO (de Jager *et al.* 1994), whereas the data above 300 GeV are from Whipple (solid box indicating total error — Weekes *et al.* 1997), HEGRA CT-system (long dashed line — average spectrum from Konopelko *et al.* 1998), and CANGAROO (short dashed box indicating total error — Tanimori *et al.* 1998). The model calculations are from de Jager *et al.* (1996), representing a variable synchrotron cutoff, as well as three steady inverse Compton spectra corresponding to the three values of σ as indicated. Reproduced from de Jager *et al.* 1996.

2.1. Basic telescope parameters, constraints and improvements

The basic requirement for a telescope is a large enough mirror collection area A_m, so that the threshold energy is a minimum. The density of Čerenkov photons produced by a γ-ray shower of energy E within a few nanoseconds at an observation depth of 830 g/m^2, is roughly (from Fig. 4 of Ong 1998)

$$\rho(E) \sim 100 E_{\rm TeV}^{1.15} \ {\rm m}^{-2}.$$

The total signal seen by a fast photon detector with quantum efficiency $\epsilon \sim 0.2$ during the Čerenkov flash, is then equal to

$$S(E) = \rho(E) A_\gamma \epsilon \sim 63 \left(\frac{r}{1 \ {\rm m}}\right)^2 \left(\frac{\epsilon}{0.2}\right) E_{\rm TeV}^{1.15},$$

photoelectrons for a mirror radius of $r = 1$ m (assuming 100% reflectivity), and assuming that the camera FOV is about 4 degrees. Such a large FOV is required to sample the shower at all angles from the incident direction, using an imaging "camera", consisting of a few hundred pixels (roughly 0.1 degree FOV per pixel).

The night sky background also produces random signals, but they can be removed by taking fast coincidences between pixels within a gate time of a few nanoseconds. It is interesting to note that the threshold energy of a present 10 meter class detector such as Whipple (see Ong 1998 for references) is only ~ 250 GeV, even though we expect ~ 50 photoelectrons from a 50 GeV γ-ray shower. Apart from aspects such as mirror quality and light guiding, the type of "off-the-rack" integrated circuits (with their own internal noise) on PC-boards usually limit gate times to ~ 10 ns and relatively large thresholds. Some reduction in threshold can be expected if one employs a solid state approach with an optimal layout to match the ~ 5 ns duration of a typical γ-ray shower. Much more effort should also be put into the production of high quantum efficiency photo detectors, such as avalanche photo diodes (APD), which can operate at $\epsilon \sim 0.8$. I forsee a solution for the problem of the internal noise of APDs, as well as the preamps to detect signals close to the single photon level with a bandwidth of a GHz. This will introduce a new dimension in γ-ray Astronomy, as well as new applications in high speed tomography in *e.g.* cancer detection and various other applications. The first applications of future γ-ray Astronomy techniques in cancer detection was achieved by the MPI für Physik in München. Once the abovementioned solutions are employed, we should see a significant shift in technology on various fronts.

2.2. Present and future γ-ray observatories

Ong (1998) lists a number of ground-based observatories which had successes in detecting γ-rays from cosmic sources. Different observational techniques are used, but the basic approaches are: (a) single stand alone telescopes, (b) telescope arrays working in stereo, (c) solar type arrays, (d) air shower arrays, and (e) under-water Čerenkov detectors. Detailed descriptions of these observatories were reported at the Kruger National Park Workshop (see *Towards a Major Atmospheric Čerenkov Detector–V*, 1997, Westprint, Potchefstroom, ed. O.C. de Jager). These Proceedings and the review of Ong also list some future experiments, which inlcude large 11 meter class telescopes working in stereo (VERITAS & HESS — ~ 40 GeV threshold), up to a single stand alone 17 meter class telescope which is aimed at a threshold of 10–30 GeV (MAGIC).

The aim of these experiments is to reduce the threshold, so that we can overlap with space experiments such as EGRET on the CGRO. We should then be able to detect the high energy tails of γ-ray bursts, see to the edge of the population of γ-ray emitting AGN, probe the pulsed emission from radio/γ-ray pulsars, and map the galactic plane in γ-rays where inverse Compton scattering is expected to dominate over the π^0 component.

Whereas the earth's magnetic field is expected to distort the images of γ-ray showers near 10 GeV to a certain degree, we still expect the angular resolution of 10 GeV showers to be much better than the ~ 1 degree resolution of EGRET in the GeV range. Not only are we gaining in resolution, but we are also gaining significantly in collection area — compare a collection of a few thousand m^2 near 10 GeV to the ~ 1 m^2 collection area of EGRET. The proton background is nearly absent below 40 GeV, whereas the electron initiated showers mimic γ-ray showers in shape — *but not in direction*, so that imaging techniques are expected to remove a significant amount of the electron and muon background. We can therefore expect to resolve/identify some of the unidentified EGRET sources with ground based techniques.

3. The Crab nebula as a standard candle

The Crab nebula (the event of AD1054) is considered to be standard candle of X-ray and γ-ray Astronomy. New telescopes/instruments are usually calibrated against the Crab. The advantage of the Crab is that it provides us with two sources at the same location for calibration purposes.

3.1. The 33 ms Crab pulsar

The Crab pulsar with period $P = 33$ ms and period derivative $\dot{P} = 422 \times 10^{-15}$ s/s provides enough spindown energy to sustain the observed plerionic emission from its surrounding nebula. The pulsar converts only a few percent of its spindown power to a broad band continuum of pulsed emission from optical to ~ 10 GeV or higher.

Nolan *et al.* (1996) detected no deviation of the pulsed intensity relative to the power law radiation component at $E > 10$ GeV. This is in contrast to the constraining upper limits placed at $E > 0.2$ TeV (see Ong 1998 for a summary). The spectrum must therefore turn over or cut off between ~ 30 and 200 GeV. The pulsed flux around 10 GeV is $\sim 10^{-4}$ photons.m^{-2}.s^{-1}, and for an expected (future) collection area of between 10^3 and 10^4 m^2 at 10 GeV, we expect between 0.1 and 1 Hz in the pulsed component. *The pulsed component can be exploited to optimise the imaging parameters for the lowest energy showers and to study the effect of the earth's magnetic field on the shape of γ-ray images.* Such studies could lead to improved angular resolution near 10 GeV.

3.2. The unpulsed nebular component

Before the discovery of pulsars, Gould (1965) exploited standard synchro-Compton theory to show that the optical/X-ray synchrotron nebula should also be responsible for the inverse Compton scattering of IR/optical photons into the TeV γ-ray range. Detectable flux levels were predicted. It was only after the employment of the atmospheric imaging technique during the 1980's, when the Whipple group reported the detection of a 20σ significant signal from the Crab nebula (Vacanti *et al.* 1991).

De Jager *et al.* (1996) have shown that the Crab nebular synchrotron spectrum, which is seen to be confined to a torus in hard X-rays, and is believed to be due to relativistic shock acceleration in the torus, should terminate around a characteristic synchrotron energy of

$$h\nu_{\max} = (\frac{3}{4\pi})^2 \frac{hc}{r_0} = 25 \text{ MeV}, \tag{2}$$

where r_0 is the classical electron radius. We see that this general maximum is independent of the electron energy and magnetic field strength in the acceleration region. This parameter-independent maximum arises from the expectation that the fastest acceleration timescale for an electron in a shock- or wave-type environment is the electron gyro period. This maximum is fundamental and was clearly detected by de Jager *et al.* as a cutoff in the EGRET spectrum of the Crab nebula. Fig. 1 shows the Crab nebular spectrum and the cutoff below $\sim$ 100 MeV is clearly seen. The component between 1 and 100 MeV is observed to be variable (de Jager *et al.* 1996), as expected from the short synchrotron lifetime of electrons with energies near 1 PeV at the pulsar wind shock, which is at a distance of ~ 0.1 pc from the pulsar.

Above this cutoff, a hard component was seen to emerge above $\sim$ 100 MeV, which may be due to the inverse Compton scattering of radio to IR emitting electrons in the Crab nebula. To claim this one must have a consistent model for the magnetic field distribution in the nebula, since a population of injected particles produce synchrotron radiation (which should match the spatially resolved synchrotron emissivity — de Jager & Harding 1992), as well as the observed high energy (HE) to very high energy (VHE) γ-ray spectrum up to multi-TeV energies. The HE to VHE spectrum was modelled to be due to inverse Compton scattering. In Fig. 1 we can see that the observed spectrum above 100 MeV is more intense than predicted by de Jager *et al.* If this component is due to inverse Compton scattering of radio to infrared emitting electrons, it would mean that the true field strength in the outer nebula is smaller than predicted by Kennel & Coroniti (1984).

The multi-TeV γ-ray spectrum of the Crab nebula also probes the inner part of the nebula, and originates from the same electron population

which radiates synchrotron hard X-rays to < 100 MeV γ-rays, except that the multi-TeV γ-rays result from IC by the same electron population. TeV Observations, more recent than those used by de Jager *et al.* (1996), confirm that $\sigma = 0.003$ (see Fig. 1). This is also consistent with the prediction by Kennel & Coroniti (1984). This "σ" parameter is the ratio of electromagnetic pressure relative to the particle pressure at the pulsar wind shock, and the change from $\sigma = 1$ to such a small value is the result of the shock formation in the relativistic pulsar wind. A low σ is also required for particle acceleration.

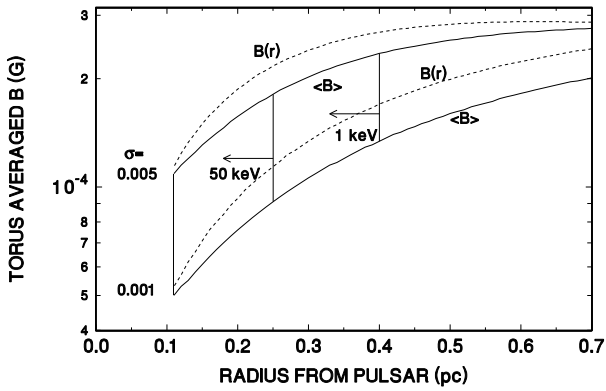

Fig. 2. The magnetic field strength of the Crab nebula as a function of radius r (in pc) from the pulsar, from the 1-D calculation of Kennel & Coroniti (1984). The field distribution depends on the σ parameter of the shock as shown by the two dashed lines. The solid lines represent the corresponding average field seen by particles confined to radii less than r. The size of the nebula at 1 keV and 50 keV are shown by the arrows. The reduction in size towards increasing energy is due to synchrotron burnoff effects.

Fig. 2 shows a plot of the field distribution $B(r)$ (from Kennel & Coroniti 1984) as a function of the radius r (1-D model) from the pulsar. Synchrotron burnoff effects confine particles between 0.1 pc and a maximum value of r, such that the particles "see" an average field $\langle B \rangle$ as indicated in Fig. 2. The size of the synchrotron nebula at a given synchrotron energy is indicated by an arrow to the left. Since the multi-TeV part of the spectrum corresponds to hard X-rays (around 50 keV), *it is clear that the multi-TeV spectrum is quite sensitive to the value of* σ, whereas the sub-TeV range should be insensitive to σ — this is also clearly seen in Fig. 1. *The observed multi-TeV spectrum therefore favours a value of* $\sigma \sim 0.003$.

However, at first glance the reader would argue that the inverse Compton spectrum cannot depend on B, which is quite true, but since we have to fix

the observed spatially resolved synchrotron (up to 50 keV) and unresolved IC spectra, we have to find $B(r)$ and the number of particles (which will also depend on r) which would satisfy all the observational constraints. Since the TeV flux is not spatially resolved, we cannot obtain a unique solution for the radial distribution of $B(r)$. We therefore force $B(r)$ from Kennel & Coroniti on the data, but leaving only σ as a free parameter. This also leaves a unique solution for $N(E)$, which would reproduce the observed spatially resolved, frequency dependent synchrotron emissivities, as well as the total observed TeV spectrum. By decreasing σ, we decrease B, so that we have to increase the number of particles to conserve the observed synchrotron spectrum. This automatically increases the expected IC flux as seen in Fig. 1.

By observing the multi-TeV spectrum of the Crab nebula, we obtain a measurement of the strength of the pulsar wind shock at a distance of 0.1 pc from the pulsar. This information is important for any model of the Crab nebular MHD flow.

4. Supernova shells as cosmic sources

High energy cosmic rays are believed to originate in the shocks of supernova shells, where the large mach number and discontinuous jump of the flow velocity across the shock create ideal conditions for the acceleration of charged particles if the shock is collissionless. With each shock crossing, the particle gains an amount of energy, which is proportional to its energy. This process continues until the acceleration timescale is longer than the fastest loss timescale, in which case the particles reach a maximum energy (see the review of Völk 1977.) In the previous section we saw how this process leads to a cutoff energy near 25 MeV for the Crab synchrotron spectrum at the pulsar wind shock, as a result of synchrotron losses.

Protons and heavier elements are expected to be accelerated by such shocks, in which case we can expect the production of very high energy cosmic rays. The detection of high energy γ-rays from SNRs by the EGRET instrument, prompted Drury, Aharonian & Völk (1994) to calculate the γ-ray spectra from these SNRs, given the normalisation provided by EGRET. A detectable component of TeV γ-rays was predicted, given the presence of molecular material in/near the SNRs, which can convert most of the energy of a proton into γ-rays. However, TeV observations of EGRET SNRs only revealed upper limits — some below predictions. Compare the predictions by Drury, Aharonian & Völk (1994) with more recent constraining TeV upper limits (Völk 1997).

4.1. W44 — a composite remnant

W44 is a radio/X-ray composite remnant with a central pulsar (PSR B1853+01, period 0.267 s) showing weak plerionic emission near the pulsar with a spectrum as indicated in Fig. 3 by the solid line labelled "PWN". The X-rays are thermal as shown by the dashed line marked "W44 (central)". The radio shell is however non-thermal synchrotron (marked "W44 (shell)" by the dot-dashed line). The radio spectrum is consistent with a power law with an index of $\alpha = 0.33$, which is harder than typical shell spectra. EGRET detected γ-rays between 70 MeV and 10 GeV from this remnant (Esposito *et al.* 1996) as shown in Fig. 3.

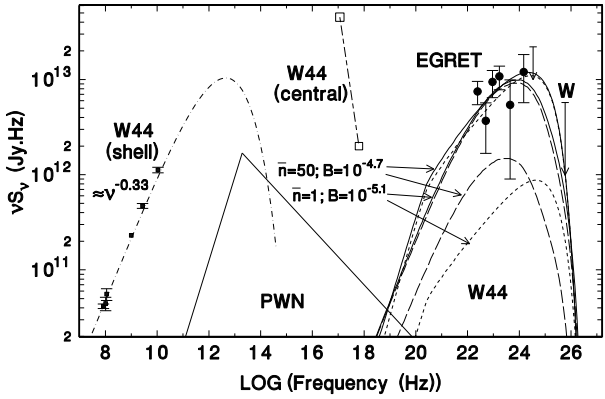

Fig. 3. The observed multiwavelength spectrum of W44 - see de Jager & Mastichiadis (1996) for references: dot-dashed line — radio synchrotron spectrum including a cutoff at $\nu_b = 3 \times 10^{12}$ Hz; open boxes — thermal X-ray energy fluxes of W44 (the thermal turnover at $\nu < kT/h$ is not included); solid circles with error bars — EGRET energy fluxes; upper limit 'W' — Whipple upper limit at $\nu = 9 \times 10^{25}$ Hz; solid triangle with base between 10^{11} Hz and 10^{20} Hz — observed radio/X-ray synchrotron spectrum of the pulsar wind nebula. The fits to the γ-ray data given two choices of the mean molecular cloud density $\overline{n}$ and shell field strength B as indicated: short dashed lines — relativistic bremstrahlung; long dashed lines — inverse Compton; thick solid lines — sum of bremstrahlung and inverse Compton. Reproduced from Mastichiadis & de Jager (1996).

De Jager & Mastichiadis (1996) took W44 as an example of a typical EGRET SNR which was not detected in TeV, so that we only have a TeV upper limit as indicated by the upper limit marked "W" (for Whipple — Lessard *et al.* 1995). De Jager & Mastichiadis have shown that the observed EGRET γ-rays may be due to relativistic bremstrahlung by radio emitting electrons in the shell. The observed steepening/cutoff between 10 GeV and TeV energies may then be due to the natural turnover/cutoff of the spectrum

of radio emitting electrons. *In fact, many of the EGRET SNRs which were thought to be due to cosmic ray proton interactions with molecular clouds, may be the result of relativistic bremstrahlung of radio emitting electrons in SNR shells, which are interacting with adjacent molecular clouds. This means that we do not yet have direct evidence for SNRs as the sources of cosmic rays such as protons and heavier elememts.*

4.2. SN1006 — a shell-type remnant

The more interesting case is when the synchrotron spectrum does not cut off in the far infrared, but rather extends towards optical/X-rays. Mastichaidis & de Jager (1996), Pohl (1996) and Yoshida & Yanagita (1997) took SN1006 as an example of shock accelertion of electrons extending to multi-TeV energies, resulting in the synchrotron bright rims seen northeast (NE) and southwest (SW) of the pulsar as seen in Fig. 4. Mastichiadis & de Jager (1996) did a detailed calculation of the time dependent shock acceleration process and showed that the best fit of the model synchrotron spectrum to the observations gives a maximum electron energy of (Eq. 6 of Mastichiadis & de Jager)

$$E_{\max} = 1.5 \times 10^7 \left(\frac{B}{f}\right) \text{ erg},$$

where B is the field strength in gauss and f is the "gyrofactor" which is defined as the particle mean free path relative to the gyroradius.

CANGAROO (Tanimori *et al.* 1998) detected TeV γ-rays only from the NE rim of the shell, but none from the SW shell. Whereas the two rims (which are at angles of less than 180 degrees relative to the center of the shell) are rougly of equal brightness in synchrotron as seen in Fig. 4, the observed differences are large at TeV energies. Various authors (Mastichiadis & de Jager 1996; Pohl 1996; Yoshida & Yanagita 1997) have shown that the IC scattering of the 2.7K cosmic microwave background by X-ray emitting electrons explains the observed γ-ray spectrum with reasonable parameters.

Fig. 5 shows the spectra of the two rims, normalised to the observed fluxes, if we interpret the TeV emission as IC as discussed above. This would imply that the magnetic field strength is larger in the SW compared to the NE, but then the number of particles have to conspire to give equal strengths in synchrotron, whereas the much smaller number of particles SW result in the non-detection at TeV energies. *By combining the synchrotron and inverse Compton spectra/observations of SNR shells, we obtain a measurement of the variation of B along the rim. However, polarisation studies which indicate the field orientation, has to be combined with shock models to see if the differences between NE and SW can be adequately explained.* Note that

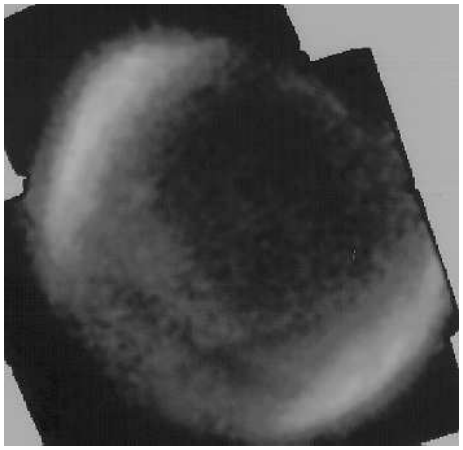

Fig. 4. ASCA image of SN1006, showing the NE (upper left) and SW (lower right) bright rims of synchrotron emission. Reproduced from the public ASCA image archives of Supernova Remnants.

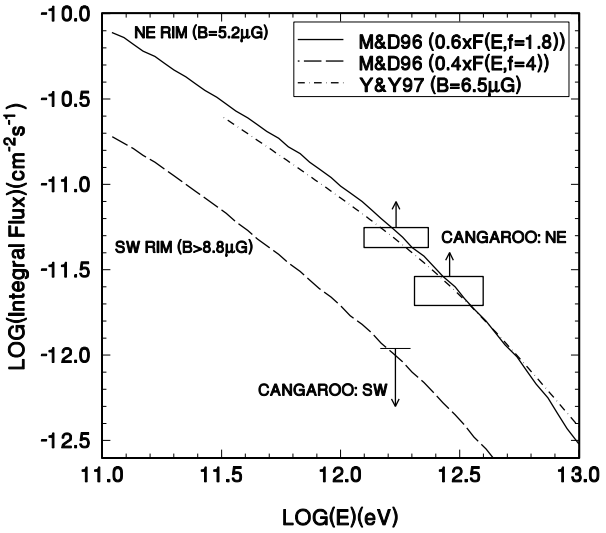

Fig. 5. The integral γ-ray flux of SN1006 as detected by CANGAROO (two solid boxes with upward arrows) from the northeastern rim (NE), as well as the corresponding upper limits for the SW rim given the non-detection. The solid- and long-dashed lines represent the spectra for the NE and SW rims respectively, with the parameters as indicated. The dot-dash line represent the mean spectrum by Yoshida & Yanagita (1997).

Mastichiadis & de Jager (1996) assumed a parallel shock configuration all around the rim, which is clearly not realistic.

Finally, we also have to revisit the possibility of π^o production in the shell of SN1006 to see if this SNR can be considered as a real cosmic ray source, rather than just another source of VHE electrons.

5. Extragalactic sources

Over 50 blazars (Active Galactic Nuclei or AGN with jets pointing towards Earth) have been detected as γ-ray sources by the Compton Gamma-Ray Observatory (see *e.g.* Thompson *et al.* 1996). Whereas the spectra extend up to 10-30 GeV, only a few AGNs have been detected at TeV energies. These are called the BL Lac objects (see Ong 1998 for a review), and are on average closer to Earth compared to other EGRET blazars. Stecker, de Jager & Salamon (1996) have made the point that X-ray selected Bl Lacs are candidates for TeV emission, since the energy output peaks towards the X-rays, whereas the radio selected BL Lacs emit lower frequency radiation on average.

A characteristic feature of AGNs in general is that you have a central black hole of $\sim 10^4$ to $\sim 10^7$ solar mass which accretes matter from the center of the host galaxy. This accretion process acts like a dynamo process, which drives a narrow jet as a result of the release of angular momentum. Since the outflow is relativistic, we see doppler shifted emission and contracted timescales as a result of the bulk flow along the jet axis. Electrons and possibly protons are accelerated in the jet (probably due to the Fermi acceleration by shocks in the jet). The electron component is again clearly visible as a synchrotron component, whereas the expected inverse Compton component may account for the observed γ-radiation.

The time variability of these sources provide an interesting diagnostic: not only do we get a measure of the size of the system from the observed timescale for variation, but we can also measure the increase of the γ-ray signal relative to its synchrotron counterpart at X-ray energies. If the relative increase in the γ-ray signal is larger than the corresponding increase in X-rays, it means that the synchrotron-self Compton process must be operational, since both the target (synchrotron) photon density (for IC scattering) and the number of electrons must have increased. The observed IC signal is then the product of the target density and the number of electrons (to a zeroth order).

Multiwavelength observations of Mkn 421 and Mkn 501 have shown correlated optical, X-ray and TeV activity (see the reviews by Petry 1997, Bradbury 1997 and Krennrich 1997). In fact, the correlation coefficient between X-rays and TeV γ-rays maximises at a time lag of $\Delta t = 0$, with $r = 0.61$,

which is very significant given all the data points considered (Aharonian *et al.* 1999). This is consistent with a synchro-Compton origin for the TeV. *The amplitudes of the TeV flares are also larger than the corresponding X-ray flare amplitudes, which hints at a "self-Compton" origin. This means that the target photon density must also be time variable, and is correlated with the X-ray intensity. This rules out a steady disk origin for the target photons.*

The 15 minute variability timescale for Mkn 421 constrain the size of the emission region to less than 10^{-4} pc (Gaidos *et al.* 1996). A similar minimum variability timescale was observed for Mkn 501 (Aharonian *et al.* 1999), and with similar doppler factors, we arrive at the same emission size, and probably black hole mass.

Since the spectrum of Mkn 501 extends to higher energies compared to Mkn 421, the effect of the intergalactic absorption was seen more clearly as a curvature in the spectrum of Mkn 501. Konopelko *et al.* (1999) have shown that the intrinsic spectrum of Mkn 501 is consistent with an E^{-2} photon spectrum. The absorption of multi-TeV photons become more pronounced above 10 TeV as a result of the intergalactic absorption of such photons by the intergalactic infrared field (Stecker & de Jager 1998).

We clearly see the effect of absorption above ~ 10 TeV from for sources at redshifts of $z \sim 0.03$. This is also expected given the minimum levels of the intergalactic infrared field density set by the ISOCAM and DIRBE/FIRAS (COBE) instruments (de Jager & Dwek 1999). *Observations above 10 GeV will certainly shift the γ-ray horison to larger redshifts, since lower energy γ-rays will need to be absorbed by UV light in the universe, of which the density is much lower compared to the IR density, resulting in larger mean free paths for 10 GeV γ-rays.*

6. Conclusions

I have only managed to scratch on the surface of ground-based γ-ray astrophysics. The present detectors operating above 100 GeV have already made significant detections and discoveries, which have enriched us beyond expectation.

By this time the reader should realise that γ-ray astronomy does not give us only one or two answers, but each new detection opens a wide range of new physics and new discoveries.

By going down to 10 GeV with next generation telescopes, we expect to increase the scientific output by at least a factor of 10, since we will overlap in energy with a space-borne instrument such as EGRET, but with the advantage of a much larger collection area, as well as better angular resolution. The latter can be quantified (and improved) by observing pulsed

γ-rays from pulsars, which should allow us to study the effects of geomagnetic deflection of the cascade development. The large rate of pulsed emission will then allow us to calibrate against geomagnetic effects as a function of position in the sky from a given location.

The Author would like to thank Prof. Francisco del Aguila and the organisers for their kind hospitality in Granada.

REFERENCES

Aharonian, F.A. *et al.*, *Astron. Astrophys.* **342**, 69 (1999).
Bradbury, S.M., in *Towards a Major Atmospheric Čerenkov Detector–V*, ed. O.C. de Jager, Westprint, Potchefstroom (South Africa) 1997, p.10.
de Jager, O.C., Harding, A.K., *Astrophys. J.* **396**, 161 (1992).
de Jager, O.C. *et al.*, *Astrophys. J.* **457**, 253 (1996).
de Jager, O.C., Mastichiadis, A., *Astrophys. J.* **482**, 874 (1996).
de Jager, O.C., Dwek, E. submitted to *Astrop. Phys.* (1999).
Drury, L.O'C., Aharonian, F.A.,Völk, H.J., *Astronom. Astrophys.* **287**, 959 (1994).
Esposito, J.A. *et al.*, *Astrophys. J.* **461**, 820 (1996).
Gaidos, J.A. *et al.*, *Nature* **383**, 319 (1996).
Gould, R.J. *Phys. Rev. Lett.* **15**, 577 (1965).
Kennel, C.F., Coroniti, F.V., *Astrophys. J.* **283**, 694 (1984).
Konopelko, A. *et al.*, to appear in *Astrophys. J. Lett.* (1999).
Konopelko, A. *et al.*, in *Rayos Cósmicos 98*, Alcalá, Spain, (1998), p.523.
Krennrich, F., in *Towards a Major Atmospheric Čerenkov Detector–V*, ed. O.C. de Jager, Westprint, Potchefstroom (South Africa) 1997, p.32.
Lessard, R.W. *et al.*, in Proc. 24th Int. Cosmic Ray Conf. (Rome) **2**, 475 (1995).
Lorenz, E., in *Towards a Major Atmospheric Čerenkov Detector–V*, ed. O.C. de Jager, Westprint, Potchefstroom (South Africa) 1997, p. 415.
Nolan, P.L. *et al.*, *Astron. Astrophys. (Suppl)* **C120**, 61 (1996).
Ong, R.A., *Phys. Rep.* **305**, 94 (1998).
Petry, D., in *Towards a Major Atmospheric Čerenkov Detector–V*, ed. O.C. de Jager, Westprint, Potchefstroom (South Africa) 1997, p.2.
Pohl, M., *Astronom. Astrophys.* **307**, 57 (1996).
Stecker, F.W., de Jager, O.C., Salamon, M.H., *Astrophys. J.* **473**, L75 (1996).
Stecker, F.W., de Jager, O.C., *Astron. Astrophys.* **334**, L85 (1998).
Tanimori, T., *et al.*, *Astrophys. J.* **497**, L25 (1998).
Thompson, D.J., *et al.*, *Astrophys. J. Suppl. Ser.*, **107**, 227 (1996).

Vacanti, G., *et al.*, *Astrophys. J.* **377**, 467 (1991).
Völk, H.J., in *Towards a Major Atmospheric Cerenkov Detector–V*, ed. O.C. de Jager, Westprint, Potchefstroom (South Africa) 1997, p.87.
Weekes, T.C., Turver, K.E., in Proc. 12th ESLAB Symp. Frascati, ESA SP-124 (1977), p. 279.
Weekes, T.C. *et al.*, *Astrophys. J.* **342**, 379 (1989).
Weekes, T.C. *et al.*, in Proc. 4th Compton Symp., Part 1, Williamsburg, (1997), p.361.
Yoshida, T., Yanagita, S., in Proc. Second INTEGRAL Workshop on the Transparent Universe ESA SP-382 (1997), p.85.